Supplement to the paper:

PACKED BED PHOTOCATALYTIC REACTORS. A PACKING STRUCTURE MODEL AND ITS EXPERIMENTAL VALIDATION WITH COMPUTERIZED TOMOGRAPHY.

by

Horacio A. Irazoqui (*), Miguel A. Isla (*), Rodolfo J. Brandi (*) and Alberto E.Cassano (*)(✉)

INTEC (**)

Universidad Nacional del Litoral and CONICET

Güemes 3450. (3000) Santa Fe. ARGENTINA

Fax: +54 – (0)342 - 4559185. E-mail: acassano@ceride.gov.ar

Key words: Photocatalysis * Packed bed reactor * Bed spatial structure * Statistical model * One particle distribution function * Two particle distribution function.

Running title: Packing structure of fixed bed photocatalytic reactors

(*) Professor at Universidad Nacional del Litoral and Research Staff Member of CONICET

(**) Instituto de Desarrollo Tecnológico para la Industria Química

(✉) Author to whom correspondence should be addressed

Abstract

The radiation field in photocatalytic packed beds results from direct energy exchange between the lamp and the catalytic beads, and from mutual exchange between beads that are close to each other. The statistical description of these exchange mechanisms requires of the knowledge of the one-particle and two-particle distribution functions. The detailed physical and mathematical basis of a statistical model of the structure of a bed of spherical-like particles of non-negligible diameter, are presented in this supplement. The proposed model has been cast in terms of one and two-particle distribution functions, based on a widely accepted physical picture of the packing structure. The model reproduces the expected bed structure surrounding arbitrarily chosen particles at different distances from the annulus walls. Elsewhere, this theoretical model has been validated against results obtained with tomography experiments.

The Reactor

The proposed device is an annular, packed bed photocatalytic reactor schematically shown Figure 1. This system shows the main features that can be found in the industrial scale reactor. The reactor bed is made of silica spheres of $d_p \approx 0.001\,\mathrm{m}$ average diameter, packed inside the annular volume between an outer $(R_e = 0.050\,\mathrm{m})$ cylinder and an inner $(R_i = 0.025\,\mathrm{m})$ concentric cylinder. The length of the catalytic bed is $L = 0.60\,\mathrm{m}$ and the annulus inner wall is masked outside this region. Layers of inert spheres (without catalytic coating) extend the packing both from the bottom of its active region downwards and from its top end upwards. This allows that a fully developed flow pattern reaches the catalytic section of the bed and avoids the need for considering end effects in the statistical description the bed structure.

If needed, for rather slow reactions, the continuous reactor operation in a partial recycle loop allows achieving large flow rates per pass without lowering the overall residence time. Larger flow rates amount to larger values of the Reynolds number defined on the basis of the superficial velocity of the fluid and the diameter of the spheres in the packed bed. In this way highly turbulent flow regimes can be achieved, minimizing the importance of mass diffusion effects through the film adjacent to the catalytic surface of the spheres. This

desirable effect brings about an increasing pressure drop along the reactor axial direction and the possibility of eroding the TiO_2 coating of the spherical beads as its counterpart.

Spatial Distribution Model for the Spheres in the Packed Bed.

The description of the lamp-to-bead exchange requires of the knowledge of the distribution of single beads in the packing, while the description of the bead-to-bead exchange requires of the knowledge of the spatial distribution of pair of beads.

A model of the spatial distribution of the spheres in the annular packed bed should necessarily account for

i) the effect of the reactor walls on the sphere spatial distribution, and
ii) the effect of the mutual volume exclusion between spheres in the close packed bed.

These two effects preclude the possibility of considering the bed as a homogeneous and isotropic packing, at least for sets of structural parameters within the range of practical interest. This is more so because the thickness of a photocatalytic annular reactor employing titanium dioxide as the catalyst is always small.

We wish to treat statistically the problem of the spatial structure of an annular packing of spherical beads. For that, we have to conceive a large number of experiments that are the same in their macroscopic details but vary in an undetermined manner in their microscopic details at a few beads level.

The experiment we may associate to the one-bead distribution consists in determining on each one of the many, macroscopically identical reactors, whether there is a sphere centered at a given position $\underline{r}_1$. This experiment will be thought of as being repeated for all feasible positions.

For each position, the ratio of the favorable outcomes to the total number of determinations performed on all the identical reactors will be expected to tend to a limit as the number of determinations tends to infinity. This limit is the probability $f^{(1)}(\underline{r}_1)\, d^{(3)}\underline{r}_1$ of a bead

having its center contained in the elementary volume $d^{(3)}\underline{r}_1$ about the generic position $\underline{r}_1$. The limit function $f^{(1)}(\underline{r}_1)$ is the one-bead distribution function.

The radiation contributions to the bead-to-bead exchange mechanism are sketched in Figure 2. The contribution to the total energy reaching the differential surface area $d^{(2)}A_1$ on the bead at the position $\underline{r}_1$, after a reflection on a differential surface area $d^{(2)}A_2$ of a neighboring bead at the position $\underline{r}_2$ is shown in Figure 2.a. The contribution due to a beam refracted and partially absorbed by the bead at the position $\underline{r}_2$ before reaching the differential surface area $d^{(2)}A_1$, is sketched in Figure 2.b. This radiation transport mechanism involves pairs of neighboring beads. Therefore, we are interested on the spatial distribution of pairs of beads.

The experiment we may associate to the distribution of pairs of beads consists in determining on each one of the many reactor replicas, whether there is a sphere centered at a given position $\underline{r}_1$ and another bead centered at $\underline{r}_2$, for every feasible pair $(\underline{r}_1, \underline{r}_2)$.

The ratio of the positive outcomes to the total number of determinations performed on all of the identical reactors is expected to tend to a limit as the number of samples tends to infinity. This limit is the joint probability $f^{(2)}(\underline{r}_1, \underline{r}_2)d^{(3)}\underline{r}_1 d^{(3)}\underline{r}_2$ of a bead having its center contained in the elementary volume $d^{(3)}\underline{r}_1$ about $\underline{r}_1$ and of another bead having its center in the elementary volume $d^{(3)}\underline{r}_2$ at $\underline{r}_2$. The limit function $f^{(2)}(\underline{r}_1, \underline{r}_2)$ is the two-bead distribution function.

Invariance Analysis and Single Reactor Statistics

Let us consider a large (though, in practice, finite), collection of macroscopically identical reactors, called reactor replicas, that differ in a random fashion from each other in the microscopic details of their packing structure.

Those properties depending exclusively on the spatial distribution of beads in the packed bed, like $f^{(1)}(\underline{r}_1)$ and $f^{(2)}(\underline{r}_1,\underline{r}_2)$, will remain unchanged when simple operations are performed on each of the replicas in the collection.

Each one of these replicas remains identical to itself at the macroscopic level, and so does their entire collection, when invariance operations like rotations around the lamp axis and (in the absence of end effects) axial translations are carried out up to an arbitrary extent.

Let's consider a pair of fixed sampling vectors $\underline{r}_1$ and $\underline{r}_2$ for each reactor replica. During the course of invariance operations, the pair of vectors associated to each one of the replicas remains unchanged, always pointing at the same spatial locations while the packing rotates and translates axially. During invariance operations the pairs of sampling vectors will sense different situations, consisting in one of the following, mutually exclusive events:

- there are simultaneously bead centers at the two locations the pair of vectors point at.
- there is a bead center around the position that one of the vectors points at, and none at the other.
- there are no centers around the positions that the pair of vectors point at.

In this work we assume that the ratio of the number of outcomes of each kind, sensed by the pair of sampling vectors, to the total number of them, will be the same irrespective on whether the ratio is computed on the entire collection of reactor replicas or on any single replica in the ensemble, subjected to the invariance operations already described. This will be more likely so if the reactor packing contains a very large number of beads, as it happens in our case.

Invariance Analysis and Independent Variables

The indifference of the values of structure-dependent properties under virtual invariance operations allows us to reduce the number of variables to be considered in the description of the problem to the minimum set of independent ones.

Lets consider the one-bead and the two-bead distribution functions depending exclusively on the packing structure. Because the packed bed consists of a cylindrical annulus

filled at random with quasi-spherical beads, both $f^{(1)}(\underline{r}_1)$ and $f^{(2)}(\underline{r}_1,\underline{r}_2)$ must remain unchanged under virtual rotations around the lamp axis keeping the sample points fixed in space.

Similarly, neglecting end effects is equivalent to assume that the packing has infinite axial length. In this is the case $f^{(1)}(\underline{r}_1)$ and $f^{(2)}(\underline{r}_1,\underline{r}_2)$ must remain invariant under arbitrary translations along the axial direction.

It is well known that in annular packed beds with $[(D_e - D_i)/d_P] > 20$ the two containing walls are far enough apart to act independently and will not simultaneously affect the beads spatial distribution[1]. The packing of our bench-scale setup fits well into this condition since $[(D_e - D_i)/d_P] \approx 25$.

In addition to this, the aspect ratio referred to the diameter of the annulus inner wall is $D_i/d_P \approx 50$, sensibly smaller than $D_i/d_P \approx 20$, which is considered the lower value of the aspect ratio for the wall curvature to have any measurable effect on the bead distribution[2].

Therefore, under our working conditions the packing can be thought of as distributed between two parallel planes separated by the distance $(R_e - R_i)$. In this limit, the annulus approaches locally the shape of an infinite slab and virtual operations like rotations around the lamp axis and axial translations become arbitrary displacements on planes parallel to the infinite slab boundaries.

On these grounds, we can impose the following invariance conditions on both $f^{(1)}(\underline{r}_1)$ and $f^{(2)}(\underline{r}_1,\underline{r}_2)$:

$$f^{(1)}(x_1, y_1, z_1) = f^{(1)}(x_1, y_1 + y_\circ, z_1 + z_\circ) \qquad (1.a)$$

$$f^{(2)}(x_1, y_1, z_1; x_2, y_2, z_2) = f^{(2)}(x_1, y_1 + y_\circ, z_1 + z_\circ; x_2, y_2 + y_\circ, z_2 + z_\circ) \qquad (1.b)$$

In Equations 1.a,b, the position vectors $\underline{r}_i, (i = 1, 2)$, have been replaced with their rectangular components (x_i, y_i, z_i), while y_o and z_o correspond to a displacement vector along an

arbitrary direction on a plane parallel to the slab boundaries. Because of the assumed arbitrariness on y_o and z_o we can always choose $y_o = -y_1$ and $z_o = -z_1$. With this choice

$$f^{(1)}(\underline{r}_1) = f^{(1)}(x_1) \tag{2.a}$$

$$f^{(2)}(\underline{r}_1, \underline{r}_2) = f^{(2)}(x_1; x_2, y_2 - y_1, z_2 - z_1) \tag{2.b}$$

Thus, with the given symmetries, $f^{(1)}(r_1)$ is a function of a single variable x_1, running along an axis perpendicular to the slab boundaries. This conclusion is valid for all packing properties depending upon a single particle position.

The symmetry analysis of $f^{(2)}(\underline{r}_1, \underline{r}_2)$ can be carried on further. Lets introduce a spherical coordinate system (ρ, θ, ϕ) centered at (x_1, y_1, z_1), with its $\theta = 0$ axis parallel to the x_1 axis of the original rectangular system and with the same direction. The following set of equations represents the transformation of one coordinate system to the other:

$$\rho = \left[(x_2 - x_1)^2 + (y_2 - y_1)^2 + (z_2 - z_1)^2\right]^{\frac{1}{2}} \tag{3.a}$$

$$\rho\cos\theta = (x_2 - x_1) \tag{3.b}$$

$$\rho\sin\theta\cos\phi = (y_2 - y_1) \tag{3.c}$$

$$\rho\sin\theta\sin\phi = (z_2 - z_1) \tag{3.d}$$

with $0 < \theta < \pi$. By substitution of Equations 3.a,b,c and d in Equation 2.b

$$f^{(2)}(\underline{r}_1, \underline{r}_2) = f^{(2)}(x_1; x_1 + \rho\cos\theta, \rho\sin\theta\cos\phi, \rho\sin\theta\sin\phi) \tag{4}$$

The function $f^{(2)}(\underline{r}_1, \underline{r}_2)$ must remain invariant when the packing, locally assimilated to a slab, revolves around the x axis by an arbitrary angle ϕ_o

$$f^{(2)}(\underline{r}_1, \underline{r}_2) = f^{(2)}[x_1; x_1 + \rho\cos\theta, \rho\sin\theta\cos(\phi - \phi_o), \rho\sin\theta\sin(\phi - \phi_o)] \tag{5}$$

Given the assumed symmetries, we can choose $\phi = \phi_o$ thus simplifying Equation 5 into the following

$$f^{(2)}(\underline{r}_1, \underline{r}_2) = f^{(2)}(x_1; x_1 + \rho \cos\theta) \tag{6}$$

where only the minimum set of independent variables has been retained. For the assumed symmetries, these results can be extended to all functions depending on the positions of pairs of beads.

The Two-Particle Distribution and the Correlation Function

The two-bead distribution function $f^{(2)}(\underline{r}_1, \underline{r}_2)$ can be written in terms of the correlation function $g(\underline{r}_1, \underline{r}_2)$ defined as follows

$$f^{(2)}(\underline{r}_1, \underline{r}_2) \equiv f^{(1)}(\underline{r}_1) f^{(1)}(\underline{r}_2) g(\underline{r}_1, \underline{r}_2) \tag{7}$$

If the event consisting in that particle "1" is at position $\underline{r}_1$ can occur irrespectively of the event that particle "2" is at the position $\underline{r}_2$, and vice-versa, the events are said to be mutually independent. If this were the case, the joint probability distribution $f^{(2)}(\underline{r}_1, \underline{r}_2)$ of the compound event consisting in that particle "1" is $\underline{r}_1$ and particle "2" is at $\underline{r}_2$, would be equal to the product of the probability distributions of the single particle events,

$$f^{(2)}(\underline{r}_1, \underline{r}_2) = f^{(1)}(\underline{r}_1) f^{(1)}(\underline{r}_2) \tag{8}$$

From Equations 7 and 8 we can conclude that the mutual independence of the events is equivalent to the condition $g(\underline{r}_1, \underline{r}_2) = 1$ for all pairs $(\underline{r}_1, \underline{r}_2)$. The condition that the beads are rigid and cannot overlap with each other makes it imposible the occurence of all pairs $(\underline{r}_1, \underline{r}_2)$ for which $\rho = \|\underline{r}_2 - \underline{r}_1\| < 2$. As a consequence of this, the equality $g(\underline{r}_1, \underline{r}_2) = 1$ cannot be satisfied for all pairs $(\underline{r}_1, \underline{r}_2)$ and the events are not independent.

By imposing the results of the invariance analysis of the preceding section on Equation 7, we obtain

$$f^{(2)}(\underline{r}_1, \underline{r}_2) = f^{(1)}(x_1) f^{(1)}(x_1 + \rho \cos\theta) g(x_1; x_1 + \rho \cos\theta) \qquad (9)$$

From Equation 9 we can see that proposing a model of $f^{(2)}(\underline{r}_1, \underline{r}_2)$ amounts to propose a model of $g(\underline{r}_1, \underline{r}_2)$, assuming that a model of the one-bead distribution function has been adopted.

The conditional probability distribution[3] $f^{(2/1)}(\underline{r}_2/\underline{r}_1)$ that particle "2" be at $\underline{r}_2$ given the certain fact that particle "1" is at the position $\underline{r}_1$, can be also be written in terms of $g(\underline{r}_1, \underline{r}_2)$

$$f^{(2/1)}(\underline{r}_2/\underline{r}_1) \equiv \frac{f^{(2)}(\underline{r}_1, \underline{r}_2)}{f^{(1)}(\underline{r}_1)} = f^{(1)}(\underline{r}_2) g(\underline{r}_1, \underline{r}_2) \qquad (10)$$

With the results of the invariance analysis of the preceding section, Equation 10, can be written as follows

$$f^{(2/1)}(\underline{r}_2/\underline{r}_1) = f^{(1)}(x_1 + \rho\cos\theta) g(x_1; x_1 + \rho\cos\theta) \qquad (11)$$

In Equations 7 and 10, the impact on the packing structure due to the walls in a finite system is described by the one-particle distribution functions $f^{(1)}(\underline{r}_1)$ and $f^{(1)}(\underline{r}_2)$, while the structure introduced by the volume exclusion effect of one particle on its surroundings is described by the two-particle correlation function $g(\underline{r}_1, \underline{r}_2)$.

The One-particle Distribution Function and the Solid Volume Fraction.

In the preceding section we have pursued the argument that the two containing walls are far enough apart to act independently and will not simultaneously affect the beads distribution at any point in the packing. At the core zone far from either wall, the beads can be assumed uniformly distributed and the limit condition

$$\lim_{x \to \infty} f(x) = n_\infty \qquad (12)$$

must be satisfied, where n_∞ is the number of bead centers per unit volume at a position x_∞ far from either wall. In Equation 12 we have dropped the label 1 of the argument x since there is no need to keep distinguishing it from any other in that way.

In the core region between the slab boundaries, n_∞ can be related to the solid volume fraction, η_∞, in a simple way

$$\eta_\infty = v_p n_\infty \qquad (13)$$

where v_P is the average bead volume.

The local solid volume fraction, $\eta(x)$, can be constructed on the basis of the one-bead distribution function[4, 5]. As shown in Figure 3.a, the beads contributing to the solid volume fraction taken at a distance $x \geq 2$ from the nearest wall are those with centers at a generic position y, such that $[(x-1) < y < (x+1)]$.

Assuming that there is a bead at that generic position, its circular area of intersection with the plane through x, parallel to the wall, is

$$A(x,y) = \pi r_P^2 \left[1 - (x-y)^2\right] \qquad (14)$$

On the other hand, the contribution of one bead located at the generic position y, to the total volume of solids contained in a elementary slab of width Δx about x, equals the product $A(x,y) \times \Delta x$, as shown in Figure 3.a.

Based on the translational invariance of the properties depending on a single particle position under arbitrary displacements on a (y,z) plane at x, we arbitrarily cut out a unit area on that plane, thus defining an elementary rectangular sampling parallelepiped of volume Δx.

The average volume of solids $\delta V_M(x)$ contained in this elementary parallelepiped when sampling a large number of (y, z) positions can be constructed by multiplying the contribution from the generic bead at y, times the probability that the bead can be found at that location, $f^{(1)}(y)\,dy$, and then integrating over the range of y, to obtain:

$$\delta V_M(x) = (r_P \Delta x) \int_{x-1}^{x+1} dy A(x,y)\, f^{(1)}(y) \qquad (15)$$

The ratio of the average solid volume in the sampling parallelepiped, $\delta V_M(x)$, to its total volume, Δx, is the local solid volume fraction:

$$\eta(x) = (\pi r_P^3) \int_{x-1}^{x+1} dy \left[1-(x-y)^2\right] f^{(1)}(y) \; ; \qquad x > 2 \qquad (16)$$

For $x < 2$ the situation is somewhat different. As it is shown in Figure 3.b, the centers of the beads in the packing cannot reach positions such that $y < 1$. This amounts to say that $f^{(1)}(y)$ must be zero for $0 < y < 1$ and no contributions to the local solid volume fraction can be expected from beads hypothetically centered in this interval. In this case

$$\eta(x) = (\pi r_P^3) \int_{0}^{x+1} dy \left[1-(x-y)^2\right] f^{(1)}(y) \; ; \qquad 0 < x < 2 \qquad (17)$$

Both of the situations just discussed can be represented by a single expression of $\eta(x)$, as follows:

$$\eta(x) = (\pi r_P^3) \int_{x-1}^{x+1} dy \left[1-(x-y)^2\right] f^{(1)}(y)\, H(y) \; ; \qquad x > 0 \qquad (18)$$

where $H(y)$ is the Heaviside step function.

The equivalent expression

$$\eta(x) = (\pi r_P^3) \int_{-1}^{1} d\zeta (1-\zeta^2) f^{(1)}(x-\zeta)\, H[(x-\zeta)-1] \; ; \qquad x > 0 \qquad (19)$$

with constant integration limits, has been obtained by substitution of $\zeta = x - y$ in Equation 18.

Although the distortion caused by the confining wall on the packing structure propagates up to about ten-bead radius distance, the direct volume exclusion effect of the wall on the beads resting against it does not affect the expression of $\eta(x)$ in terms of $f^{(1)}(y)$ for $x \geq 2$. This situation is accounted for by Equation 19 because for $x \geq 2$ and $(-1 < \zeta < 1)$, we always have $[(x-\zeta)-1] \geq 0$, and consequently, $H[(x-\zeta)-1] = 1$. Therefore, we have

$$\eta(x) = (\pi r_P^3) \int_{-1}^{1} d\zeta \, (1-\zeta^2) f^{(1)}(x-\zeta) \quad ; \qquad x \geq 2 \qquad (20)$$

Equations 19 and 20 are integral relationships between the solid volume fraction and the one particle distribution function. If $f^{(1)}(x)$ is known the local solid volume fraction can be calculated. Conversely, if $\eta(x)$ is known, Equations 19 and 20 are integral equations in the unknown function $f^{(1)}(x)$.

General Features of a Model of the One-particle Distribution Function

A statistical model of randomly packed beds must put together the distinctive features of this type of packing. In particular, the mathematical form of $f^{(1)}(x)$ must be consistent with the physical picture summarily described as follows:

A lower bound greater than $x_o \approx 1$ can be imposed on x_o due to the fact that a spatial configuration with x_o close to one is considered very unlikely, given the compactness of the first layer of a packing under practical conditions[6-8].

To estimate an upper bound for x_o, we may consider the extreme situation in which the beads in the first layer are at close packing conditions, where every bead is surrounded and touched by other six beads of the same layer. Under these circumstances, the closest position to the wall that the center of a bead in the second layer can reach is that which corresponds to the bead resting on three beads belonging to the first layer.

The centers of these four beads at contact with each other forms a regular tetrahedral. If we call this distance x_{cp}, then for looser structures the range of x_o can be conservatively estimated to be $[1 < x_o < x_{cp}]$, noting that a bead in the second layer never reaches the lower bound. From standard trigonometry calculations we find that $x_{cp} = 2.633$.

The subsequent layers are less and less ordered. The wall effects on the particle distribution weakens and it oscillates about its asymptotic value in a damped fashion until at the core region between the slab boundaries the beads can be assumed uniformly distributed.

The mathematical form of $f^{(1)}(x)$ must bring together the main aspects of the physical picture just described. This picture can be summarily phrased as follows:

- There is a highly ordered and fairly compact first layer with most of the beads resting against the nearest wall[6-8]. This is the most meaningful statistical event regarding this first layer, and the one-bead distribution function must express the certainty that most of the beads in this layer have their centers on a plane at $x = 1$, parallel to the wall.

- Moving from the wall inwards a second layer, not so well defined as the first one, is found. Most of the beads of this second layer rest on the ones of the first layer. Therefore, there is a direct volume exclusion effect from beads in the first layer upon those of the second one. The number of bead centers per unit volume corresponding to the second layer starts building up only beyond a distance x_o depending on the average bead concentration. In the interval $[1 < x < x_o]$, going from the plane of centers of the first bead layer to the position x_o, no bead centers can be found due to the exclusion effect already discussed. From the statistical standpoint, this amounts to say that $f^{(1)}(x)$ must be zero in the interval $[1 < x < x_o]$.

- At x_o the first few centers are found belonging to those beads in the second layer that reach closer to the wall. At this point, the value of the one particle distribution function and that of its derivative should equal zero, both increasing in a continuous fashion with x in the vicinity of x_o.

- Subsequent layers are less and less ordered. The wall effects on the particle distribution weakens and it oscillates about its asymptotic value in a damped fashion until, at the core region between the slab boundaries, the beads can be assumed to be uniformly distributed.

On these grounds we conclude that there are two, mutually exclusive events to take into account when modeling the one bead distribution function $f^{(1)}(x)$: the sample bead at x either belongs to the first layer, in which case $x = 1$, or to the subsequent, less ordered layers with its center at $x > x_\circ$.

We propose the following expression of $f^{(1)}(x)$:

$$f^{(1)}(x) = C\,\delta(x-1) + H(x-x_\circ)\,\varphi(x) \quad ; \; 1 < x_\circ < x_{cp} \tag{21}$$

The first term of Equation 21 corresponds to the probability density that a bead can be found at the distance $x = 1$ from the wall, which is a certain fact. Aside for the constant C related to the compactness of the first layer, this term consist of the Dirac delta "function" $\delta(x-1)$ which is zero everywhere except at $x = 1$, where it is unbounded. Among other properties, the delta "function" has the following one

$$\delta(y-y_\circ)h(y) = \delta(y-y_\circ)h(y_\circ) \tag{22}$$

where $h(y)$ is an arbitrary function, continuous at $y = y_\circ$.

The second term of Equation 21 is a product of the Heaviside step function $H(x-x_\circ)$ times a continuous damped oscillating function $\varphi(x)$. The step function models the direct volume exclusion effect of the first layer on the next one. On the other hand, the damped oscillating function is consistent with the physical picture in which the local concentration of bead centers oscillates about its asymptotic value in a damped fashion as the wall effects on the packing structure weakens, to finally approach a uniform distribution.

As it was discussed above, at $x_\circ$ the value of the one particle distribution function and that of its derivative should be zero, therefore

$$\varphi(x_\circ) = 0 \tag{23.a}$$

and

$$\varphi'(x_\circ) = 0 \tag{23.b}$$

From Equations 19 and 21, the corresponding expression of $\eta(x)$ in terms of $\varphi(x)$ is

$$\eta(x) = C\,\pi r_P^3 \left[1 - (x-1)^2\right] H(2-x)\,H(x) + \\ + \pi r_P^3 \int_{-1}^{1} d\zeta \left(1-\zeta^2\right)\varphi(x-\zeta)\,H[(x-\zeta)-x_\circ] \tag{24}$$

Considering that experimental values of $\eta(1)$ are widely reported in the literature for the most frequent random loose packing conditions, the substitution of $x = 1$ in Equation 24, gives

$$C = \left(\frac{\eta(1)}{\pi r_P^3}\right) - \int_{-1}^{1-x_\circ} d\zeta \left(1-\zeta^2\right)\varphi(1-\zeta) \quad ; \quad 1 < x_\circ < 2 \tag{25.a}$$

$$C = \left(\frac{\eta(1)}{\pi r_P^3}\right) \quad ; \quad x_\circ > 2 \tag{25.b}$$

Equations 25.a;b help to estimate the value of C for the purpose of the presentation of the model, and also to check the consistency of our own experimental results to be presented in the next paper of this series. Assuming the values $x_\circ \approx 2$; $\eta(1) \approx 0.77$ and $r_p \approx 5.0\times10^{-4}\,\mathrm{m}$ hold in our case, we find that $C \approx 1.96\times10^{9}$ beads/m^3.

For $x \geq (x_\circ + 1)$ Equation 24 becomes

$$\eta(x) = \pi r_P^3 \int_{-1}^{1} d\zeta \left(1-\zeta^2\right)\varphi(x-\zeta) \quad ; \quad x \geq (x_\circ + 1); \quad 1 < x_\circ < x_{cp} \tag{26}$$

because under these conditions $H[(x-\zeta)-x_\circ] = 1$ in the entire range of ζ, $[-1 < \zeta < 1]$.

At distant locations from either wall the packing structure tends to be uniform and Equation 26 tends to the limit expression

$$\eta_\infty = \left[\pi r_P^3 \int_{-1}^{1} d\zeta \left(1-\zeta^2\right) \right] \varphi_\infty = v_P \varphi_\infty \qquad (27)$$

By comparison of Equation 13 with Equation 27, we conclude that

$$\varphi_\infty = n_\infty \qquad (28)$$

Equation 28 is an asymptotic condition that the function φ must satisfy in addition to the constraints of Equations 23.a, b.

A Mathematical Model of the One Particle Distribution Function

From the physical analysis of the precedent section we conclude that the general features that the one particle distribution must have are expressed in Equations 21 to 23. A mathematical form should be proposed for the damped oscillating function $\varphi(x)$, consistent with the fact that the local concentration of bead centers oscillates about its asymptotic value in a damped fashion with x, to finally approach a uniform distribution. We propose for $\varphi(x)$ the following expression

$$\varphi(x) = n_\infty \left\{ 1 + e^{-bx} \left[c_1 \cos(ax) + c_2 \sin(ax) \right] \right\} \quad ; \quad (a,b) > 0 \qquad (29)$$

where b is the damping coefficient, a is the frequency of the oscillation and c_1 and c_2 are constants. The expression for $\varphi(x)$ of Equation 29 satisfies the asymptotic condition of Equation 28.

The mathematical form proposed for the function φ must also satisfy the constraints of Equations 23.a, b. It is easy to show that these constraints can be expressed as follows

$$c_1 \cos(ax_\circ) + c_2 \sin(ax_\circ) = -e^{bx_\circ} \qquad (30.a)$$

$$c_1 \sin(ax_\circ) - c_2 \cos(ax_\circ) = \frac{b}{a} e^{bx_\circ} \qquad (30.b)$$

where $x_\circ$ is the parameter defined in Equations 21 to 23.

Solving the system of Equations 30.a, b for c_1 and c_2 in terms of a, b and $x_\circ$, we obtain

$$c_1 = e^{bx_\circ}\left[\left(\frac{b}{a}\right)\sin(ax_\circ) - \cos(ax_\circ)\right] \qquad (31.a)$$

$$c_2 = -e^{bx_\circ}\left[\sin(ax_\circ) + \left(\frac{b}{a}\right)\cos(ax_\circ)\right] \qquad (31.b)$$

Substitution of Equations 31.a, b in Equation 29, after a rearrangement, gives

$$\varphi(x) = n_\infty - n_\infty e^{-b(x-x_\circ)}\left\{\cos[a(x-x_\circ)] + \left(\frac{b}{a}\right)\sin[a(x-x_\circ)]\right\}; \quad (x > x_\circ) \qquad (32)$$

The expression of $\varphi(x)$ in Equation 32 satisfies the constraints of Equations 23 and 28; and when replaced in Equation 21 completes the mathematical model of the one particle distribution function. The result is shown in Figure 4 for a set of parameters taken from literature[2].

By substitution of Equation 32 in Equation 24 we obtain the expression of $\eta(x)$consistent with the model proposed for $f^{(1)}(x)$. For values of $x_\circ$ in different intervals, the resulting equation embodies all the particular situations encountered as the value of x increases in the interval $(1 < x < \infty)$. All the situations arising in this process are thoroughly discussed in Appendix I, supported on its complement Appendices II and III. The values of $\eta(x)$ as predicted by the model Equations 24 and 32 are shown in Figure 5 for the same parameter values as those of Figure 4. The parameters in Equations 21 and 32 will be determined by non-linear regression of tomography experiments[9].

The Radiation Field and the Two-Particle Distribution Function

As it was discussed earlier in this work, the rate of photocatalytic reactions on a "test" bead differential area will depend on the useful energy per unit time and unit area reaching a reaction site either from the lamp or from neighboring beads. A statistical model of the packed bed structure based on the probability of occurrence of pairs of beads is an indispensable supporting tool for the simulation of the energy exchange between a test bead and its surroundings.

The prevailing direct two-body energy exchange is a short-range phenomenon. This is so because this mechanism involves the "test" particle at the generic position $\underline{r}_1$ and those in the shell of nearest neighbors, their position being collectively represented by $\underline{r}_2$.

This nearest couch of beads includes:

- Those beads at contact with the "test" particle, even if they fail to complete a surrounding compact shell, and

- Those beads that, although not stricktly at contact with the "test" particle, still are close enough to it so that its circular cross section can be seen from reaction sites on the central bead surface.

This couch acts as a screen preventing radiation from those beads in outer shells to have direct access to the surface of the "test" particle. As a consequence of this, all the particles effectively participating in the direct energy exchange with a central "test" particle have their centers inside a sphere of radius ρ_{nc}, enclosing all surrounding beads which participate in the radiation exchange with the central bead catalytic surface.

A conservative upper bound of ρ_{nc} can be easily calculated if we assume that the beads surrounding the central one were close packed. In this case, we may consider the arrangement made of the central bead, together with three of the beads at contact with it and with each other, and a fifth bead at contact with these last three beads. In this compact arrangement, the fifth bead is the more distant one from the central bead that still can be seen from points on the test particle surface, although mostly eclipsed by the beads at the intermediate positions.

The five bead centers are the vertices of two regular tetrahedra with a common triangular face. The distance between the two vertices farther apart in this arrangement is the closest distance of approach of a particle in the second surrounding layer to the central one, under close packing conditions. From standard trigonometry calculations we find that this distance is $\rho_{cp} = 3.266$. For looser arrangements, we have $2 < \rho_{nc} < \rho_{cp} = 3.266$. The radius ρ_{cp} thus defined is a very conservative upper bound for the radius of the nearest surrounding couch, ρ_{nc}.

Beyond that distance, direct two-body radiation exchange contributions from beads located farther away from particle 1 would be unduly taken into account. Therefore, both $f^{(2)}(\underline{r}_1,\underline{r}_2)$ and $g(\underline{r}_1,\underline{r}_2)$ can be considered short-range functions assumed to be zero outside a sphere of radius ρ_{nc}.

The Two-bead Correlation Function in Packings of Spherical Beads

The model adopted for the two-bead correlation function for loose-packed beads has been thoroughly discussed elsewere[9]. Here, we are going to highlight the key arguments on which the model is based.

- For a liquid of rigid spheres, the radial distribution function from statistical mechanics shows the general mathematical form found for randomly packed spheres[10]. But since the results from statistical theories of classical fluids are not applicable without further considerations to packing densities as high as those of a loose packed bed, quantitative agreement cannot be expected.

- A large body of numerical simulations has given strong evidence for the adequacy, over an extensive range of parameters, of various approximate integral equations for the pair correlation function in classical fluids. The simplest of these, and on the basis of comparisons against numerical simulations, the most satisfactory, is the approximate Percus-Yevick (PY) theory[11].

- A close form of the pair correlation function $g(\rho;\eta)$ for a homogeneous and isotropic fluid of rigid spheres was obtained by Wertheim[12] as the solution of the PY integral

equation. The Wertheim (W) solution behaves satisfactorily beyond the range of η for which the approximations on which the PY equation is based are considered valid, and is able to approximate results of numerical simulations up to mass fractions close to that of the liquid-solid transition of rigid spheres systems.

- Because of the volume exclusion effect of the central particle on its surroundings, the two-particle correlation function must be zero in the interval $(0 < \rho < 2)$, irrespective on whether the system is homogeneous and isotropic or not. Beyond $\rho = 2$ the W analytic solution for the case of an infinite, isotropic medium is expressed in the form

$$g(\rho;\eta) = \sum_{n=1}^{\infty} g_n(\rho;\eta) \qquad (33)$$

where the dependence of the pair correlation function on the uniform solid volume fraction has been made explicit.

- A generic n-th term, $g_n(\rho;\eta)$, in Equation 33 behaves as follows

$$g_n(\rho;\eta) = 0 \quad ; \rho < 2n \quad \text{or} \quad \rho > 2n \qquad (34.a)$$

$$g_n(\rho;\eta) > 0 \quad ; 2n < \rho < 2n+2 \qquad (34.b)$$

these conditions were obtained for $n = 1,2,...\infty$. The interpretation of Equations 34.a,b is that for a given ρ, only one term of Equation 33 is different from zero, namely the one whose label satisfies the condition $2n < \rho < 2n+2$, with n an integer number. As a result of this, Equation 33 offers a description of $g(\rho;\eta)$ in terms of concentric layers, each one relieving the preceeding layer as ρ increases in the interval $(2 < \rho < \infty)$.

- Except for its core region free from wall effects, our packing differs from those systems for which the pair correlation function has been derived, in that it is neither uniform nor isotropic. Besides, the asymptotic solid volume fraction in this region is expected to be $\eta_\infty \approx 0.62$, well inside the solid phase region of an isotropic and homogeneous system of

rigid spheres, and halfway between η_{LS} and η_{CP}, which are the values of the solid volume fraction at the liquid-to-solid transition, and at close packing, respectively.

- The W close expression of $g(\rho;\eta)$ is not applicable as a predicting tool to packing densities as high as those found in loose packed beds. Outside the range of η where the theory is valid, the W mathematical form of the pair correlation will be used as a sensible expression on which to lay a model of the first layer surrounding a central bead in the narrow band $(2.0<\rho<\rho_{nc})$, and for the dimensionless densities η of interest here.

- As part of our model, we will assume that the exclusion effect of the central bead on its nearest neighbors propagates along each direction through its non-homogeneous immediate surroundings, as it would have done in a hypothetical homogeneous and isotropic medium with a solid volume fraction η^*, different for each one of the directions considered. The solid volume fraction η^* for every feasible direction will be chosen as the local value of η in the structured medium, taken at the halfway position between the center of the test bead, x_1, and that of its closest neighbor, $x_1+\rho\cos\theta$, along every θ direction of search.

- With this choice, η^* will depend on the direction considered as follows

$$\eta^* = \eta\left(x_1+\frac{1}{2}\rho\cos\theta\right)\ ; \qquad 2<\rho<\rho_{nc};\ 0<\theta<\pi \tag{35}$$

- In previous sections, we have argued that only those pairs of beads with distance between centers, ρ, in the interval $\left[2<\rho<\rho_{nc}<\rho_{cp}=3.266\right]$ are provisionally considered to account for the bead-to-bead energy exchange mechanism. Therefore, for our purposes in this work, only the first layer contribution to the W expression of $g(\rho;\eta^*)$ will be retained,

$$g(\rho;\eta^*)=g_1(\rho;\eta^*) \tag{36}$$

- The expression of $g_1(\rho;\eta)$ according to the W solution is given elsewere[9] and its profiles for different values of η are shown in Figure 6. For the largest values of the parameter η^*, it may happen that the downward slope following the sharp peak at $\rho = 2$ is so steep that $g(\rho_{min};\eta^*)$ reaches a relatively small and negative value. This unphysical situation is corrected by requiring that $g(\rho;\eta)$ be always positive or zero.

With this model of the pair correlation function in the packed bead, and the symmetry considerations made in previous paragraphs, Equation 9 may be written

$$f^{(2)}(x_1; x_1 + \rho\cos\theta) \approx f^{(1)}(x_1)\, f^{(1)}(x_1 + \rho\cos\theta)\, g(\rho;\eta^*) \qquad (37)$$

where $2 < \rho < \rho_{nc}$ and $0 < \theta < \pi$.

The conditional probability distribution $f^{(2/1)}(x_1 + \rho\cos\theta/x_1)$ that bead 2 is at $x_2 = x_1 + \rho\cos\theta$ given the certain fact that bead 1 is at the position x_1, may also be written in terms of $g(\rho;\eta^*)$

$$f^{(2/1)}(x_2/x_1) = f^{(2/1)}(x_1 + \rho\cos\theta/x_1) \approx f^{(1)}(x_1 + \rho\cos\theta)\, g(\rho;\eta^*) \qquad (38)$$

Equation 38 completes our model for the statistical description of the packed bed structure based on the probability of occurrence of single beads and of pairs of beads. In the following section, the structure of the packed bed in terms of pair of beads as the present model predicts it will be discussed.

The Packing Structure in Terms of Pair of Beads. Analysis of Conditional Probability Profiles.

The conditional probability $f^{(2/1)}(x_1 + \rho\ \cos\theta\ /x_1)$ as a function of θ in the interval $(0 < \theta < \pi)$, for several constant values of the position of the central bead, x_1, and of the radial distance, ρ, can be represented in polar coordinates. The length of the radius vector in

this representation is proportional to the value of the function $f^{(2/1)}$, and the $\theta = 0$ direction is collinear with the x_1 axis.

Figure 7 corresponds to the arbitrary "test" particle (particle 1) resting against the containing wall (i.e., $x_1 = 1$). In this case, the conditional distribution function, $f^{(2/1)}$, is zero for values of θ in the interval $[(\pi/2) < \theta < \pi]$. This is so because for $x_1 = 1$ and for values of θ in this interval, the distance of bead 2 to the wall,

$$x_2 = x_1 + \rho\cos\theta \tag{39}$$

will be, if not negative, smaller than unity, for any positive ρ. As we know, this is a situation incompatible with the fact that beads can not be found at a distance to the wall shorter than unity, when measured as multiple of one bead radius.

The factor $f^{(1)}(x_2)$ in Equation 38, has the mathematical form given by Equation 21. For $x_2 < x_\circ$, it becomes

$$f^{(1)}(x_2) = C\,\delta(x_2 - 1) \tag{40}$$

The substitution of Equation 40 in Equation 38, gives

$$f^{(2/1)}(x_2/x_1) \approx C\,\delta(x_2 - 1)\; g(\rho;\eta^*) \tag{41}$$

where η^* has been defined in Equation 35. The Dirac δ "function" with argument $(x_2 - 1)$ will be zero everywhere, except at $x_2 = 1$, where it is unbounded. From Equation 39 it can be seen that, for $x_1 = 1$, this happens at $\theta_1 = \pi/2$ and, as a consequence, $x_2 = x_1 = 1$. This result is shown in Figure 7 by means of spikes pointing at opposite directions as icons representing the unbounded Dirac δ "function".

From a physical standpoint, the meaning of this singularity of the conditional probability at $\theta_1 = \pi/2$ is that there are beads in the nearest couch surrounding the central particle, which are precisely at a distance $x_2 = 1$ from the containing wall.

Always keeping the central particle at $x_1 = 1$, we can see that the inequality $1 < (x_2 = 1 + \rho\cos\theta) < (\rho + 1)$ holds for values of θ in the interval $[0 < \theta < (\pi/2)]$. For given values of $\rho \geq 2$, there will be some values of θ for which the calculated location of the surrounding bead, x_2, is in the interval $[1 < x_2 < x_\circ]$, where no bead centers can be found. Therefore, the $f^{(2/1)}$ function should be zero for these values of θ, as it can be seen in Figure 7.

If the chosen value of ρ is greater than $(x_\circ - 1)$, in the process of θ going through values from $\theta = \pi/2$ to $\theta = 0$, the distance of the surrounding bead to the wall, x_2, begins to be larger than $x_\circ$ at an angle $\theta = \theta_\circ$, and the $f^{(2/1)}$ function begins to show non-zero values. In Figure 7, the value of $\theta_\circ$ corresponds to the slope of the straight line through the origin, which also is a tangent to the considered ρ = constant profile.

For $\theta < \theta_\circ$, the conditional probability $f^{(2/1)}$ increases with decreasing θ, until a maximum is reached. Then it decreases to a minimum at $\theta = 0$.

The local maxima of $f^{(2/1)}$ as a function of θ, correspond to the angular positions of the surrounding particles in the most probable structure around the test particle at $x_1 = 1$, i.e., that with surrounding beads at $\theta = \pi/2$, which are also resting against the wall, and other surrounding beads at a $\theta \approx \pi/4$ angle.

The model also accounts for the fact that not all the particles in the nearest surrounding couch are at contact with the "test" particle (i.e., at a relative distance $\rho = 2$), but some of them are at distances a bit larger. The shrinking profiles of Figure 7 with $\rho > 2$ reflect this possibility, although the conditional probability associated to these events decays sharply as ρ increases, revealing a rather thin layer.

Figure 8 corresponds to cases where the "test" particle is located at different distances from the wall. These positions were chosen within the interval $[1 < x_1 < 3]$, and the profiles correspond to situations where the bead "2" is at contact with the central bead $(\text{i.e., } \rho = 2)$. The corresponding most probable structures surrounding the central particle have been sketched on the left half field of the same figure.

Although the details are different, the arguments used in the discussion of the profiles of Figure 7 are applicable to the profiles of Figure 8.

In this case, the conditional distribution function, $f^{(2/1)}$, is zero for values of θ in the interval $[(\pi/2) < \theta_1 < \theta < \pi]$, with $\rho \cos\theta_1 = (1 - x_1)$ and $\rho = 2$. This is so because for values of θ in this interval, the distance of bead 2 to the wall calculated from Equation 39 will be less than unity, which is an unphysical situation.

For $\theta = \theta_1$, $x_2 = 1$ and the Dirac δ "function" in Equation 41 becomes unbounded. As before, this result is shown in Figure 8 by means of spikes tilted by an angle θ_1, which is different for each location of the central bead.

Again, the physical interpretation of this result is that there are beads in the nearest couch surrounding the central particle, which are precisely at a distance $x_2 = 1$ from the containing wall, as long as $x_\circ < x_1 < 3$.

For θ values a bit smaller than θ_1, the distance of particle "2" to the wall, x_2, as given by Equation 39 will be in the range $1 < x_2 < x_\circ$, which is an unphysical situation. This will happen as θ decreases, until the value $\theta_\circ$ is reached for which $x_\circ = x_1 + \rho\cos\theta_\circ$; i.e., the position of particle "2" has just reached the innermost margin of the gap in the bead centers distribution due to the volume exclusion effect of the beads resting against the wall. For values of θ lower than $\theta_\circ$, the conditional probability $f^{(2/1)}$ assumes non-zero values, with its local maxima corresponding to the most probable angular positions of bead "2" in the immediate surroundings of particle "1". The angles $\theta_\circ$ and θ_1 are shown in Figures 8.a, b, c, d.

Figure 9 corresponds to the case where the "test" particle is located at a radial position $x_1 = 10$, rather distant from the wall.

Considering the ρ=constant contours of Figure 9 we can conclude that local maxima and minima are more evenly distributed with θ than for positions closer to the wall, approaching the limit circular shapes we expect to find in the homogeneous core region of the packing.

The lack of symmetry of the contours about the $\theta = \pi/2$ direction is due to the fact that the perturbation introduced by the wall still affects the distribution of the spheres, even though it decays as the distance from the wall becomes larger. This is the reason why the "test" particle "sees" different structures along directions at supplementary values of θ. In fact, the profiles are more structured for $\pi/2 < \theta < \pi$, closer to the wall, than for their suplementary counterparts in the range $0 < \theta < \pi/2$, closer to the core region.

Conclusions

A model of the one-bead distribution function has been proposed on the basis of a large body of scientific results from literature. It offers a statistical description of the bed structure in terms of single particles, which is consistent with the singular nature of the layer of beads resting against the containing walls, as well as with the volume exclusion effect they exert on neighboring bead layers. Farther from the wall, it reproduces the expected damped oscillating behaviour until the uniform, random core region is reached.

When calculated in terms of the proposed one-bead distribution function, the solid volume fraction increases in a quasi-parabolic fashion, starting from zero at the wall and reaching a first local maximum at about one bead radius distance from the wall, while a sharp minimum is attained at about two bead radius distance from it.

Once the model of the one-bead distribution has been adopted, proposing a model of the two-particle distribution function is equivalent to propose a model of the pair correlation function. For this, we have borrowed from statistical mechanics the close form of the pair distribution function for a homogenous and isotropic system of rigid spheres obtained as the solution of the integral Perckus-Yevick equation, tested valid for solid volume fractions up to

0.47, corresponding to the liquid-solid transition. With some restrictions, in the non-homogeneous packing this function is evaluated for the solid volume fraction found halfway between the centers of the two particles.

The pair distribution function introduces naturally the mutual exclusion effect between rigid particles, as well as the structure of the first shell of neighbors surrounding a given particle and its dependence on the degree of compactness of the bed.

The model reproduces the expected bed structure at the surroundings of an arbitrarily singled-out particle at different radial distances from the containing walls.

In a following paper, the model has been validated against results obtained with tomography experiments.

Acknowledgments

Thanks are given to Universidad Nacional del Litoral (CAI+D 96-0017-120 and Project N° 39 (Program 6)), FONCYT (BID 802/OC-AR: PID 95-022, PICT 97-13-00000-01209 and PICT 2000-14-10055) and CONICET (PIP 98-0205) for financial help. The permanent financial assistance of Universidad Nacional del Litoral and CONICET are gratefully acknowledged.

Nomenclature

a	frequency factor, dimensionless
b	damping coefficient, dimensionless
c_1	constant defined in Equation 31.a, dimensionless
c_2	constant defined in Equation 31.b, dimensionless
$d^{(2)}A_i$	differential surface area at the position $\underline{r}_i$, dimensionless
$d^{(3)}\underline{r}_i$	elementary volume at the position $\underline{r}_i$, dimensionless
$f^{(1)}(\underline{r}_1)$	probability distribution of one bead with its center at position $\underline{r}_1$, m^{-3}
$f^{(2)}(\underline{r}_1, \underline{r}_2)$	probability distribution of pair of beads, m^{-6}
$g(\underline{r}_1, \underline{r}_2)$	correlation function defined in Equation 7, dimensionless
$H(x)$	Heaviside step function.
L	useful length of the catalytic bed, m
n_∞	bead centers per unit packing volume in the core region, m^{-3}
R_e	external radius of annular bed (=D_e/2), m
R_i	internal radius of annular bed(=D_i/2), m
r_p	average bead radius (= d_p /2), m
$\underline{r}_i$	position vector with components (x_i, y_i, z_i) in a rectangular frame of reference
$\underline{r}_{21}$	position of bead 2 relative to that of bead 1
v_P	average bead volume, m^3
x	rectangular coordinate running along an axis perpendicular to the slab walls and increasing from either inwards, measured as a multiple of the average bead radius, dimensionless
x_o	distance from where the second layer starts, dimensionless
x_{cp}	distance from the wall to the perfectly ordered second layer under close-packing conditions, dimensionless
x_∞	values of x in the region far from the walls and around the midpoint between the slab boundaries, dimensionless
y	generic position of the center of a bead, dimensionless
$y_\circ$	arbitrary displacement from (x, y, z) along the y coordinate axis on a $x=$

constant plane, dimensionless

z_o arbitrary displacement from (x,y,z) along the z coordinate axis on a $x=$ constant plane, dimensionless

Greek Symbols

$\delta(x)$ Dirac delta "function"

$\eta(x)$ local solid volume fraction at the position x, dimensionless

η_∞ mass volume fraction in the uniform core region, dimensionless

η_{cp} mass volume fraction of a close-packed homogeneous arrengement, dimensionless

η_{LS} mass volume fraction at the liquid-to-solid transition, dimensionless

$\varphi(x)$ oscillating function defined in Equation 29.

ζ variable of integration, dimensionless

(ρ,θ,ϕ) spherical coordinate system centered at (x_1,y_1,z_1), with its $\theta=0$ axis collinear to the x axis of the rectangular system

ρ distance from the center of bead 1 to the center of bead 2 measured as a multiple of the average bead radius, dimensionless

ρ_{cp} distance from the center of the "test" particle to that of a bead in a second surrounding layer under close packing conditions, dimensionless

ρ_{nc} radius of the sphere enclosing the nearest couch of beads surrounding a central particle, dimensionless.

References

(1) Mueller, G. *Radial Void Fraction Correlation for Annular Packed Beds. AIChE J.* **1999,** *45*(11), 2458.

(2) Martin, H. *Low Peclet Number Particle-Fluid Heat and Mass Transfer in Packed Beds. Chem. Eng. Sci.* **1978**, *33*, 913.

(3) Kolmogorov, A.N. *Foundations of the Theory of Probability.* Chelsea Publishing Company: New York, 1956, Chap I, p. 6.

(4) Kubie, J. *Ph. D. Thesis.* The University of Aston in Birmingham, 1974.

(5) Kubie, J. *Influence of Countering Walls on the Distribution of Voidage in Packed Beds of Uniform Spheres. Chem. Eng. Sci.* **1988**, *43*(6),1403.

(6) Ridgway, K. and Tarbuck, K.J. *Radial Voidage Variation in Randomly Packed Beds of Spheres of Different Sizes. J. Pharm. Pharmac.* **1966,** *18*, Suppl. 168S.

(7) Ridgway, K. and Tarbuck, K.J. *Voidage Fluctuations in Randomly-packed Beds of Spheres Adjacent to a Containing Wall. Chem. Eng. Sci.* **1968**, *23*, 1147.

(8) Govindarao, V.M.H. and Froment, G.F. *Voidage Profiles in Packed Beds of Spheres. Chem. Eng. Sci.* **1986**, *41*(3), 533.

(9) Irazoqui, H. A.; Isla, M. A.; Brandi, R. J. and Cassano, A. E.. *This journal*, **2003**.

(10) Scott G.D., Charlesworth A. M., and Mak M. K.*On the Random Packing of Spheres. J. Chem. Phys.* **1964**, 40, 2, 611.

(11) Balescu R. *Equilibrium and Nonequilibrium Statistical Mechanics*, John Wiley & Sons.: New York, 1975, Chap. 3.

(12) Wertheim M. S. *Exact Solution of the Percus-Yevick Integral Equation for Hard Spheres. Physical Review Letters* **1963,** *10*(8), 321.

Appendix I:

The compact expression of $\eta(x)$ consistent with the model proposed for $f^{(1)}(x)$:

$$\eta(x) = \pi r_P^3 \; C(x_\circ)\left[1-(x-1)^2\right] \; H(2-x)H(x) + \\ + \pi r_P^3 \int_{-1}^{1} d\zeta \left(1-\zeta^2\right)\varphi(x-\zeta)\, H[(x-\zeta)-x_\circ] \qquad \text{(I.1)}$$

embodies every particular situation that can be encountered as the value of x increases in the interval $[1 < x < \infty]$.

The function $\varphi(x)$ appearing in Equations I.1 is an analytic expression given in Equation 32.

Based on the properties of the Heaviside step function, in this Appendix we will unfold this general expression into the different forms it acquires over the feasible ranges of $x_\circ$ and x.

From its definition

$$H(y) = \begin{cases} 1 \; ; & y > 0 \\ 0 \; ; & y < 0 \end{cases} \qquad \text{(I.2)}$$

Therefore, we may conclude that the integral term in Equation I.1 will be non-zero only for those values of x such that $(x - x_\circ) > -1$, for a given x_o in the interval $[1 < x_\circ < x_{cp}]$. Assuming that this condition is satisfied, the integral will effectively extend from $\zeta = -1$ to either $\zeta = (x - x_\circ)$ or $\zeta = 1$ as its upper limit, whichever occurs first as ζ increases in the integration interval $[-1 < \zeta < 1]$.

In this Appendix, every particular form that Equation I.1 will be discussed.

Case 1: For $0 < x < 2$ and $(x - x_\circ) < -1$, we have $H(2 - x)\,H(x) = 1$ and the integral term in Equation I.1 is zero. In this case, the expression of $\eta(x)$ reduces to

$$\eta(x) = \pi r_P^3\, C\left[1 - (x-1)^2\right] \tag{I.3}$$

Case 2: For $0 < x < 2$ and x and x_0 such that $-1 < (x - x_\circ) < 1$, the integral of Equation I.1 is non-zero and it extends from $\zeta = -1$ to $\zeta = (x - x_\circ)$. The corresponding expression of $\eta(x)$is:

$$\eta(x) = \pi r_P^3\, C\left[1 - (x-1)^2\right] + \pi r_P^3 \int_{-1}^{x-x_\circ} d\zeta \left(1 - \zeta^2\right)\varphi(x - \zeta) \tag{I.4}$$

In this case, the maximum value that the integral upper limit, $(x - x_\circ)$, can have is unity.

Case 3: For $x > 2$ and $x_\circ$ such that $-1 < (x - x_\circ) < 1$, we have $H(2 - x)\,H(x) = 0$ and the expression of $\eta(x)$ is

$$\eta(x) = \pi r_P^3 \int_{-1}^{x-x_\circ} d\zeta \left(1 - \zeta^2\right)\varphi(x - \zeta) \tag{I.5}$$

Case 4: Increasing the value of x beyond $(1 + x_\circ) > 2$, we have $H(2-x)\,H(x) = 0$ and $(x - x_\circ) > 1$. The corresponding expression of $\eta(x)$ is

$$\eta(x) = \pi r_P^3 \int_{-1}^{1} d\zeta \left(1 - \zeta^2\right)\varphi(x - \zeta) \tag{I.6}$$

All these cases can be easily sorted out with the aid of logical program statements. The integrals appearing in the different mathematical forms of $\eta(x)$ corresponding to each one of the cases discussed are closed, analytical expressions calculated in Appendices II and III.

Appendix II:

In the interval $[-1 < (x - x_\circ) < 1]$, we have

$$\int_{-1}^{1} d\zeta \left(1-\zeta^2\right)\varphi(x-\zeta)\, H[(x-\zeta)-x_\circ] = \int_{-1}^{(x-x_\circ)} d\zeta \left(1-\zeta^2\right)\varphi(x-\zeta) \qquad \text{(II.1)}$$

for a given $x_\circ$ in the interval $[1 < x_\circ < x_{cp}]$.

Direct integration of Equation II.1, performed after substitution of the expression of $\varphi(x-\zeta)$ obtained from Equation 26, gives

$$\int_{-1}^{(x-x_\circ)} d\zeta \left(1-\zeta^2\right)\varphi(x-\zeta) = n_\infty\left[\frac{2}{3}+(x-x_\circ)-\frac{(x-x_\circ)^3}{3}\right] - \frac{e^{-b[1+(x-x_\circ)]}}{a\left(a^2+b^2\right)^2}\left\{c_1\cos[a(x-x_\circ)]+c_2\sin[a(x-x_\circ)]\right\} \quad ; \quad -1<(x-x_\circ)<1 \qquad \text{(II.2)}$$

where

$$c_1 = c_{11}\cos(a) + c_{12}\sin(a) \qquad \text{(II.3.a)}$$

$$c_2 = c_{21}\cos(a) + c_{22}\sin(a) \qquad \text{(II.3.b)}$$

and

$$c_{11} = (-2a)\left[\left(a^2+b^2\right)+2b\right] \qquad \text{(II.4.a)}$$

$$c_{12} = 2\left[-b\left(a^2+b^2\right)+\left(a^2-b^2\right)\right] \qquad \text{(II.4.b)}$$

$$c_{21} = c_{12} \qquad \text{(II.4.c)}$$

$$c_{22} = -c_{11} \qquad \text{(II.4.d)}$$

The expressions above have been worked out from the results obtained using the free-access QuickMath Automatic Math Solutions (www.quickmath.com).

We are also interested on the integral

$$\int_{-1}^{1} d\zeta \left(1-\zeta^2\right)\varphi(1-\zeta)\, H[(1-\zeta)-x_\circ] = \int_{-1}^{(1-x_\circ)} d\zeta \left(1-\zeta^2\right)\varphi(1-\zeta) \qquad \text{(II.5)}$$

with $-1 < (1 - x_\circ) < 1$. The result of this integration can be obtained substituting $x = 1$ in Equation II.2.

Appendix III:

We are interested on the integral

$$\int_{-1}^{1} d\zeta \,(1-\zeta^2)\varphi(x-\zeta)\, H[(x-\zeta)-x_\circ] = \int_{-1}^{1} d\zeta \,(1-\zeta^2)\varphi(x-\zeta) \qquad \text{(III.1)}$$

for $(x - x_\circ) > 1$ and $[1 < x_\circ < x_{cp}]$.

Direct integration of Equation (III.1), with $\varphi(x-\zeta)$ obtained from Equation 32, gives

$$\int_{-1}^{1} d\zeta \,(1-\zeta^2)\varphi(x-\zeta) = n_\infty\left(\frac{4}{3}\right) -$$
$$n_\infty \frac{e^{-b[1-(x-x_\circ)]}}{a\left(a^2+b^2\right)^2}\left\{d_1\cos[a(x-x_\circ)] + d_2\sin[a(x-x_\circ)]\right\} + \qquad \text{(III.2)}$$
$$n_\infty \frac{e^{-b[1+(x-x_\circ)]}}{a\left(a^2+b^2\right)^2}\left\{d_3\cos[a(x-x_\circ)] + d_4\sin[a(x-x_\circ)]\right\}$$

where

$$d_i = d_{i1}\cos(a) + d_{i2}\sin(a) \qquad ; \quad i = 1,2,3,4 \qquad \text{(III.3)}$$

and

$$d_{11} = (-2a)\left[\left(a^2+b^2\right) - 2b\right] \qquad \text{(III.4.a)}$$
$$d_{12} = 2\left[b\left(a^2+b^2\right) + \left(a^2-b^2\right)\right] \qquad \text{(III.4.b)}$$
$$d_{21} = -d_{12} \qquad \text{(III.4.c)}$$
$$d_{22} = d_{11} \qquad \text{(III.4.d)}$$
$$d_{31} = (2a)\left[\left(a^2+b^2\right) + 2b\right] \qquad \text{(III.4.e)}$$
$$d_{32} = 2\left[b\left(a^2+b^2\right) - \left(a^2-b^2\right)\right] \qquad \text{(III.4.f)}$$
$$d_{41} = d_{32} \qquad \text{(III.4.g)}$$

$$d_{42} = -d_{31} \qquad \text{(III.4.h)}$$

This expression has been worked out from the results obtained using the free-access QuickMath Automatic Math Solutions (www.quickmath.com).

Figure Captions:

Figure 1: Reactor configuration

Figure 2: Contributions to the bead-to-bead exchange mechanism. Figure 2.a sketches the contribution to the total energy reaching the differential surface area $d^{(2)}A_1$ on the bead at the position $\underline{r}_1$, after a reflection on a differential surface area $d^{(2)}A_2$ of a neighboring bead at the position $\underline{r}_2$. Figure 2.b illustrates the contribution due to a beam refracted and partially absorbed by the bead at the position $\underline{r}_2$ before reaching the differential surface area $d^{(2)}A_1$.

Figure 3: The feasible locations, y, of beads contributing to the solid volume fraction $\eta(x)$. Figure 3.a: when x is at a distance $x \geq 2$ from the nearest wall, beads located in the interval $[(x-1) < y < (x+1)]$ contribute. Figure 3.b: when $x < 2$, the contributing beads are located in the interval $[1 < y < (x+1)]$, since there are no beads in the packing at positions $y < 1$. Therefore $f^{(1)}(y)$ must be zero for $0 < y < 1$.

Figure 4: The one-bead distribution function $f^{(1)}(x)$as a multiple of n_∞according to the proposed model (Equations 21, 31 and 32), with a = 3.85; b = 0.25; $x_\circ = 1.8$; $C = 1.96 \times 10^9$ (beads/m^3); and $n_\infty = 1.184 \times 10^9$ (beads/m^3) as tentative values of the parameters.

Figure 5: The solid volume fraction $\eta(x)$ resulting from the proposed model of $f^{(1)}(x)$. The values of the parameters are as in Figure 4.

Figure 6: The pair distribution function $g(\rho;\eta)$ for $\eta_\infty = 0.62$ and $0 < \rho < 4$.

Figure 7: The conditional probability $f^{(2/1)}$ for $x_1 = 1$, represented in polar coordinates as a function of θ, for several constant values of ρ $(\rho = 2.00;\ 2.1;\ 2.2;\ \text{and} 2.3)$. The length of the radius vector is proportional to the dimensionless value $\left(f^{(2/1)} / n_\infty\right)$ for each corresponding pair (θ, ρ). The values of the parameters are as in Figure 4.

Figure 8: The conditional probability $f^{(2/1)}$ for different "test" particle locations in the interval $(1 \leq x_1 \leq 3)$ and corresponding sketches of the most probable structure around the central bead.

Figure 9: The conditional probability $f^{(2/1)}$ represented in polar coordinates as a function of θ, for several constant values of ρ $(\rho = 2.00;\ 2.1;\ 2.2;$ and $2.3)$. The "test" particle has been located at a radial position $x_1 = 10.$.

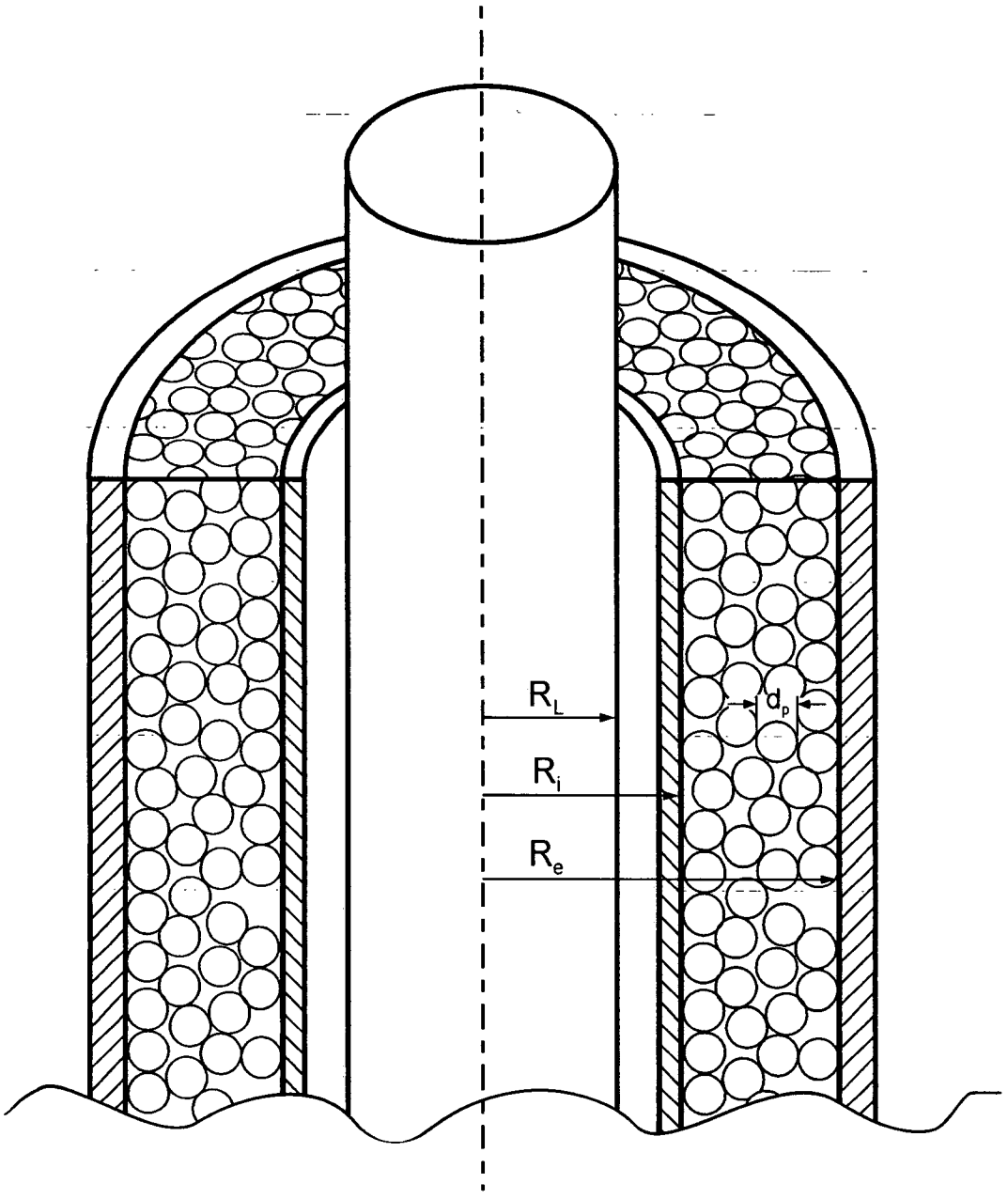

Figure 1
(Irazoqui et al. sup)

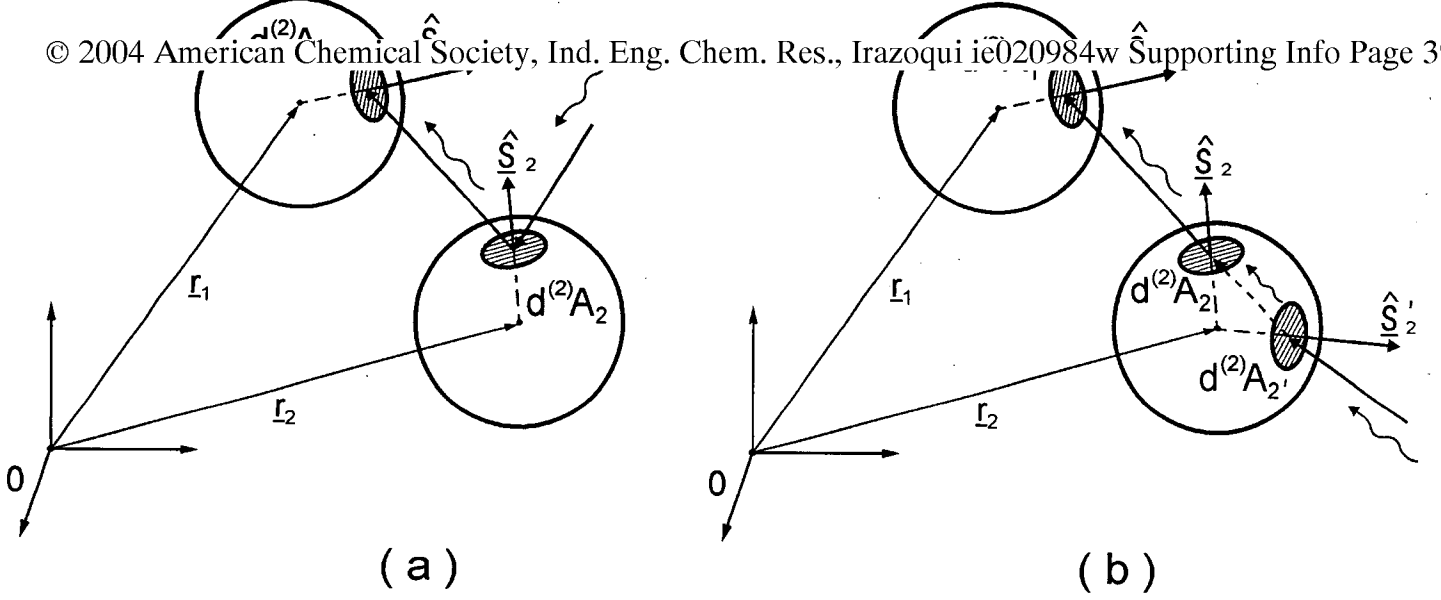

Figure 2
(Irazoqui et al.

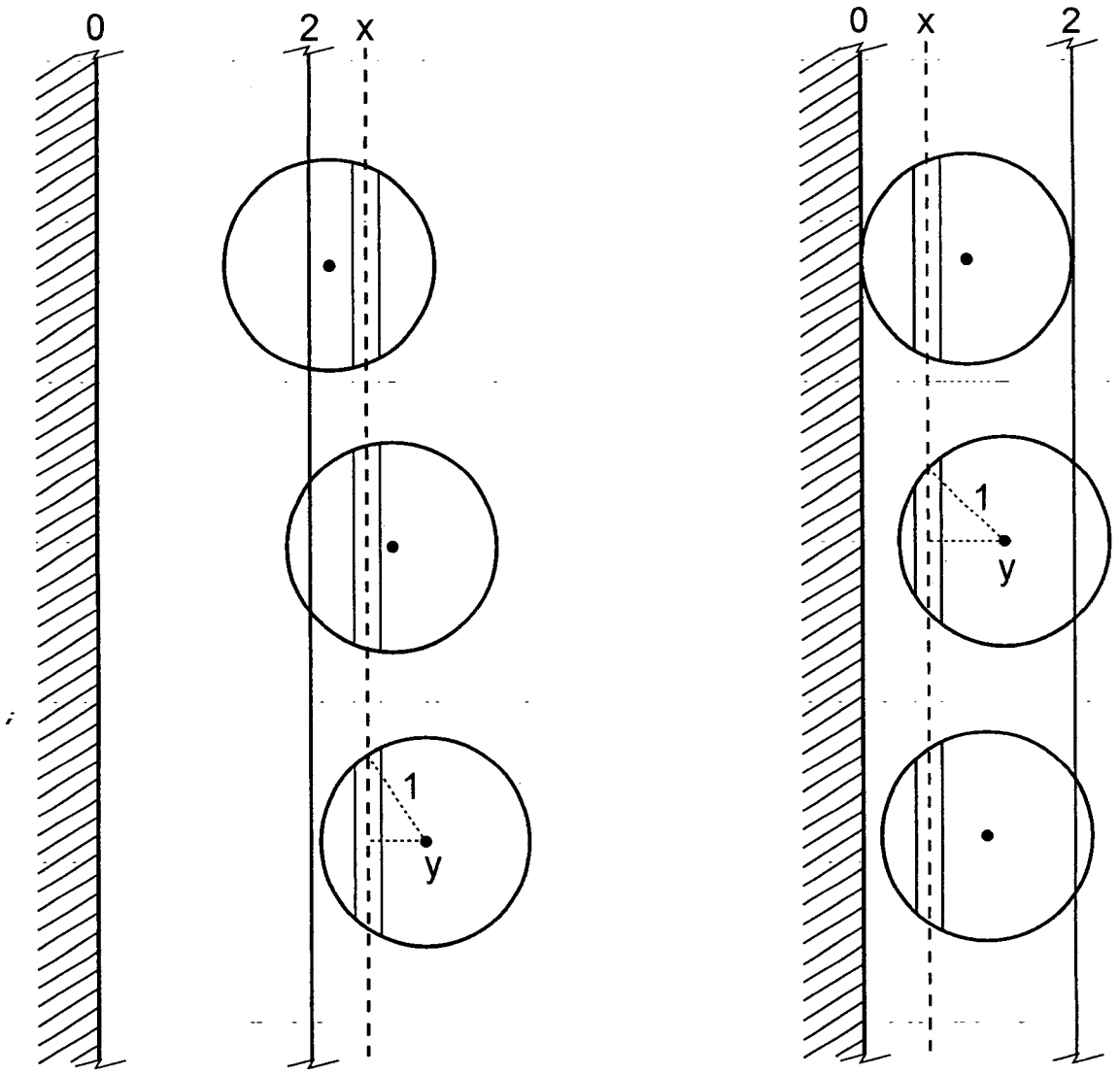

Figure 3
(Irazoqui et al. sup.)